



Quantum Monte Carlo study of the cooperative binding of NO₂ to fragment models of carbon nanotubes

John W. Lawson^{a,*}, Charles W. Bauschlicher Jr.^b, Julien Toulouse^c, Claudia Filippi^{d,e}, C.J. Umrigar^f

^a NASA Ames Research Center, Space Technology, Mail Stop 229-1, NASA Ames Research Center, Moffett Field, CA 94035, USA

^b Mail Stop 230-3, NASA Ames Research Center, Moffett Field, CA 94035, USA

^c Laboratoire de Chimie Théorique, Université Pierre et Marie Curie and CNRS, Paris, France

^d Instituut-Lorentz, Universiteit Leiden, P.O. Box 9506, NL-2300 RA, Leiden, The Netherlands

^e Faculty of Science and Technology and MESA+ Research Institute, University of Twente, P.O. Box 217, 7500 AE Enschede, The Netherlands

^f Laboratory of Atomic and Solid State Physics, Cornell University, Ithaca, NY 14853, USA

ARTICLE INFO

Article history:

Received 18 August 2008

In final form 17 October 2008

Available online 26 October 2008

ABSTRACT

Previous calculations on model systems for the cooperative binding of two NO₂ molecules to carbon nanotubes using density functional theory and second order Moller–Plesset perturbation theory gave results differing by 30 kcal/mol. Quantum Monte Carlo calculations are performed to study the role of electronic correlations in these systems and resolve the discrepancy between these previous calculations. Compared to QMC binding energies, MP2 and LDA are shown to overbind, while B3LYP and BPW91 underbind. PW91 gives the best agreement with QMC with a binding energy differing by only 3 kcal/mol. Basis set effects are also shown to be important.

Published by Elsevier B.V.

1. Introduction

Understanding the interaction of molecular adsorbates with carbon nanotubes (CNT) is important for many applications. Recent experimental work [1] for example showed a two orders of magnitude increase in the conductivity of a semiconducting CNT after exposure to small amounts of gaseous NO₂. These results suggest that CNTs might be utilized as very sensitive molecular sensors. The mechanism for this phenomenon remains unclear with explanations ranging from charge transfer between the adsorbate and the nanotube to modifications of interface barriers at the contacts. The viability of a charge transfer mechanism depends on the nature of the bonding between an adsorbate and a nanotube. In particular, formation of a chemical bond may be necessary to enable significant charge transfer to occur.

Ab initio calculations by Ricca and Bauschlicher (RB) [2] based on density functional theory (DFT), second order Moller–Plesset perturbation theory (MP2), and coupled cluster singles and doubles calculations including the effect of connected triples determined using perturbation theory [CCSD(T)] examined the interactions of NO₂ molecules with (9,0) and (10,0) carbon nanotubes. Based on MP2 calculations of NO₂ on coronene, they estimated the binding energy of a single NO₂ molecule to a carbon nanotube to be roughly 5 kcal/mol, where binding energies are defined as the energy of the free constituents minus the energy

of the composite system. The weak nature of this binding argues against a charge transfer mechanism.

Another interesting possibility is that two NO₂ molecules might attach to neighboring carbons on the tube. In this scenario, the breaking of the π bond between two carbons could make the formation of two C–NO₂ bonds energetically favorable [3]. To consider this possibility, RB [2] performed DFT calculations using the B3LYP functional and a small 6-31G* basis on nanotubes with periodic boundary conditions (PBC). They found a binding energy of two NO₂ molecules to be –2 kcal/mol for the (9,0) metallic nanotube and –10 kcal/mol for the semiconducting (10,0) tube. Similar periodic calculations performed using a plane wave basis and the PW91 functional [4] obtained binding energies of 4 and –6 kcal/mol for two NO₂ on (9,0) and (10,0) nanotubes, respectively.

However, DFT is known to perform poorly in situations involving weak binding. To assess the error in their DFT numbers, RB [2] examined smaller model systems extracted from large tube geometries. These systems were sufficiently small to permit calculations using larger basis sets and more accurate correlated quantum chemistry methods. The use of DFT, MP2, and CCSD(T) gave very different answers for the binding energy, with results differing over a range of 30 kcal/mol. We note that the accuracy of DFT for CNT-adsorbate problems was also investigated in Ref. [5] where the binding of a single O₂ molecule to a CNT was also studied with quantum Monte Carlo (QMC) techniques. For this weakly bound complex, the local density approximation (LDA) was found to give better agreement with QMC than the PBE generalized gradient approximation.

* Corresponding author.

E-mail address: John.W.Lawson@nasa.gov (J.W. Lawson).

In this Letter, we use quantum Monte Carlo (QMC) to calculate the binding energies and the bonding geometries for the reduced models developed in Ref. [2] to describe the binding of two NO₂ molecules to a carbon nanotube. These models exhibit complex interactions (electrostatic, van der Waals, π - π interactions, etc.) that are representative of a broad class of CNT-adsorbate problems. While DFT (often with small basis sets) is the method of choice for calculations involving full nanotubes due to their large size, the significant spread of binding energies found by RB [2] when using different ab initio approaches for the reduced models indicate that correlation effects play an important role. We choose QMC to investigate these correlation effects and assess the performance of other theoretical approaches in describing these systems. QMC enjoys a more favorable scaling with system size compared to conventional highly correlated quantum chemistry methods, and therefore it has a considerable advantage as the models we consider contain up to 108 electrons and the computations are therefore quite demanding.

2. Method

We employ two quantum Monte Carlo (QMC) methods [6,7]. First the variational Monte Carlo (VMC) method is used to compute the energy expectation value of an optimized trial wave function. Second, starting from this optimized wave function, the fixed-node diffusion Monte Carlo (DMC) method is used to project onto the ground state subject to the constraint that the nodes of the projected wave function are the same as those of the trial wave function.

The N -electron trial wave function $\Psi_T(\mathbf{R})$ has the form

$$\Psi_T(\mathbf{p}, \mathbf{R}) = J(\boldsymbol{\alpha}, \mathbf{R}) \sum_{i=1}^{N_{\text{CSF}}} c_i C_i(\boldsymbol{\lambda}, \mathbf{R}), \quad (1)$$

where $\mathbf{R} = (\mathbf{r}_1, \dots, \mathbf{r}_N)$ represents the $3N$ electron coordinates, $\boldsymbol{\alpha}$ are the Jastrow parameters and $J(\boldsymbol{\alpha}, \mathbf{R}) = e^{f(\boldsymbol{\alpha}, \mathbf{R})}$ is a Jastrow factor with $f(\boldsymbol{\alpha}, \mathbf{R})$ a sum of two body (electron–electron, electron–nucleus) and three body (electron–electron–nucleus) correlation terms. The electron–nucleus and the electron–electron–nucleus Jastrow parameters are different for each atom type. The configuration state functions (CSF's), $C_i(\boldsymbol{\lambda}, \mathbf{R})$, are symmetry adapted linear combinations of Slater determinants built from single-particle orbitals $\psi_{\mu}(\mathbf{r}) = \sum_{\nu=1}^{N_b} \lambda_{\mu,\nu} \chi_{\nu}(\mathbf{r})$ which in turn are expanded on a set of basis functions $\{\chi_{\nu}(\mathbf{r})\}$. The total set of possible variational parameters \mathbf{p} consist of those for the Jastrow parameters, $\boldsymbol{\alpha}$, the CSF coefficients \mathbf{c} , the orbital coefficients $\boldsymbol{\lambda}$, and the exponents of the basis functions [8]. The wave function parameters $\mathbf{p} = (\boldsymbol{\alpha}, \mathbf{c})$ were optimized using recently developed energy minimization methods [9–11], that have been shown to perform significantly better than the standard variance minimization algorithm [12]. The orbital coefficients $\boldsymbol{\lambda}$ and the basis exponents were kept fixed.

Monte Carlo integration is used to estimate the variational energy

$$E_{\text{VMC}} = \frac{\langle \Psi_T | \hat{H} | \Psi_T \rangle}{\langle \Psi_T | \Psi_T \rangle} = \frac{1}{M} \sum_m E_L(\mathbf{R}_m) + O(1/\sqrt{M}), \quad (2)$$

where $E_L(\mathbf{R}) = H\Psi_T(\mathbf{R})/\Psi_T(\mathbf{R})$ is the local energy and the Monte Carlo points, \mathbf{R}_m , are sampled from a probability distribution $|\Psi_T(\mathbf{R})|^2 / \int d\mathbf{R} |\Psi_T(\mathbf{R})|^2$ using an accelerated version [13] of the Metropolis–Hastings algorithm [14,15]. The variational theorem guarantees that E_{VMC} is an upper bound for the ground state energy.

The second step in a QMC computation is diffusion Monte Carlo (DMC). In DMC, the optimized trial wave function $\Psi_T(\mathbf{R})$ is evolved according to the integral representation of the Schrodinger equation in imaginary time

$$\Psi_T(\mathbf{R})\Psi(\mathbf{R}, t + \tau) = \int G(\mathbf{R}, \mathbf{R}', \tau) \Psi_T(\mathbf{R}')\Psi(\mathbf{R}', t) d\mathbf{R}', \quad (3)$$

where $G(\mathbf{R}, \mathbf{R}', \tau)$ is an approximation to the importance-sampled Green function $\Psi_T(\mathbf{R})\Psi_T^{-1}(\mathbf{R}') | e^{-\hat{H}\tau} | \mathbf{R}' \rangle$. In the limit $\tau \rightarrow \infty$, $\Psi(\mathbf{R}, t + \tau)$ will approach the true ground state. In practice the projection is subjected to the fixed-node constraint which gives the best wave function that has the same nodes as the trial wave function. The resulting fixed-node DMC energy is an upper bound to the ground state energy if the potential is local. The ‘fixed-node error’ is the principal error in a DMC computation. It can be greatly reduced by optimizing the determinantal parameters \mathbf{c} , $\boldsymbol{\lambda}$ and the basis exponents in the presence of the Jastrow factor. Although the Jastrow factor does not by itself affect the location of the nodal surface, it has an indirect effect on the nodal surface because the optimal determinantal parameters depend on the Jastrow parameters $\boldsymbol{\alpha}$. Optimizing the variational parameters also reduces other less important systematic errors in DMC, as well as, the statistical error for a given number of Monte Carlo steps. The DMC algorithm has a time-step error due to the use of an approximate $G(\mathbf{R}, \mathbf{R}', \tau)$. We employ a DMC algorithm [16] that takes into account the singularities in $G(\mathbf{R}, \mathbf{R}', \tau)$ and has a small time-step error.

We employed both single determinant and multideterminant trial wave functions. The single-determinant wave functions were constructed from B3LYP orbitals using GAMESS [17]. Simultaneous optimization of the orbital coefficients and basis exponents together with the Jastrow and CSF coefficients can be done using energy minimization methods [10,18], but in this work we kept the orbital coefficients fixed at their B3LYP values. The large size of the systems makes such calculations prohibitive.

We use norm-conserving sp -non-local effective core potentials (ECP) for carbon, nitrogen and oxygen, generated in all-electron Hartree–Fock calculations for the atoms [19]. These ECPs are finite at the nucleus and are therefore more suitable for QMC calculations with a Gaussian basis than are other singular ECPs commonly used in quantum chemical calculations. They avoid divergences in the local energy when an electron approaches the nucleus since the orbitals expressed on an atomic Gaussian basis do not exactly

Table 1

Binding energies (BE) (kcal/mol) for Ndown and Odown calculated by DFT, MP2, and QMC using 6-31G*, cc-pVTZ, and ECP basis sets as indicated. The Ndown/Odown energy difference is $\Delta = E_{\text{Odown}} - E_{\text{Ndown}}$ (kcal/mol). Binding energies are positive for bound systems. QMC statistical error on binding energies is 1 kcal/mol.

	BE(Ndown)	BE(Odown)	Δ
<i>All-electron calculations</i>			
B3LYP/6-31G*	–29.2	–22.6	–6.6
BPW91/6-31G*	–26.0	–23.3	–2.7
PW91/6-31G*	–14.2	–12.7	–1.5
LDA/6-31G*	18.6	10.9	7.7
MP2/6-31G*	–9.3	–11.6	2.3
B3LYP/cc-pVTZ	–36.5	–30.2	–6.3
BPW91/cc-pVTZ	–33.6	–31.2	–2.4
PW91/cc-pVTZ	–22.5	–21.1	–1.4
LDA/cc-pVTZ	12.3	4.3	8.0
MP2/cc-pVTZ	–7.9	–12.9	5.0
<i>All-electron symmetrized models [2]</i>			
CCSD(T)/6-31G*	–18.9		
<i>ECP calculations</i>			
HF	–69.0	–48.3	–20.8
B3LYP	–37.5	–30.9	–6.6
MP2	–9.4	–13.8	4.4
<i>Single determinant/ECP QMC</i>			
VMC	–25.3	–38.5	13.2
DMC	–19.4	–18.2	–1.3
<i>Multi CSF/ECP QMC</i>			
VMC			9.4
DMC			–2.5

satisfy the electron–nucleus cusp condition. The potential of the hydrogen atom is also softened by removing the Coulombic divergence following the construction given in [20]. This potential reproduces the exact s eigenvalue of -0.5 Hartree to better than 10^{-4} Hartree. Note however that the hydrogen ECP does not reduce the number of electrons. The orbitals in the determinantal component of the wave functions are expanded in contracted Gaussian basis sets (11s11p2d)/[4s4p2d] for carbon and nitrogen, (12s12p2d)/[5s5p2d] for oxygen, and (11s2p)/[3s2p] for hydrogen. The approximate treatment of the non-local ECPs in DMC [21] results in an ECP ‘locality error’ that is reduced by using well optimized trial wave functions.

QMC calculations have smaller basis-size errors than do most other quantum chemistry methods. The basis set, used in our QMC calculations, has better than valence triple zeta (VTZ) quality. The B3LYP and MP2 binding energies using this basis are in good agreement with the binding energies obtained from all-electron calculations using the (cc-pVTZ) basis set of Dunning and coworkers [22], the largest difference being 1.5 kcal/mol (see Table 1).

3. Model

The geometries for our calculations were taken from the work of Ricca and Bauschlicher [2], who constructed (9,0) and (10,0) carbon nanotubes in periodic cells and studied them using various DFT functionals and basis sets, and different bonding configurations depending on the orientation of the two NO_2 molecules. The (9,0) CNT was further studied using short capped tubes (C_{150} and C_{186}) optimized at the BPW91/4-31G level of theory. From the C_{150} tube, reduced models were extracted that included the adsorbates and a curved piece of the tube consisting of 16 carbon atoms. Dangling bonds were passivated with hydrogen atoms. We consider here three of their reduced models. We call ‘Ndown’ (see Fig. 1) the bonding configuration where both NO_2 molecules have their nitrogen atoms bonded to the nanotube.

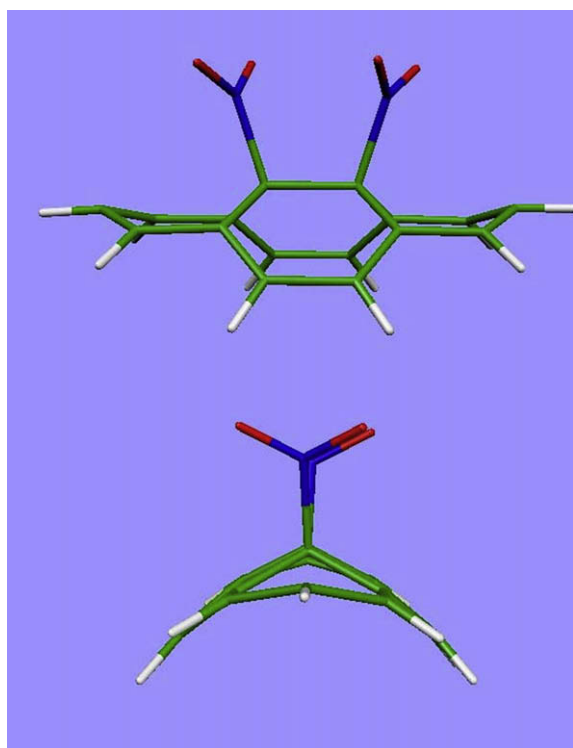


Fig. 1. Bonding configuration for NO_2 called ‘Ndown’ where the N atoms are bonded to the nanotube model fragment.

tion called ‘Odown’ (see Fig. 2) has one oxygen per molecule bonded to the tube. The puckering of the carbon atoms near the adsorption sites shows the local effect of the adsorbates on the tube. The third system is a curved piece of nanotube without the adsorbates that we loosely call ‘pyrene’. After removing the core electrons through the use of ECPs, NO_2 has 17 electrons, pyrene has 74 electrons and Ndown and Odown each have 108 electrons.

It is important to note several aspects of our reduced models. Firstly, the geometries have not been reoptimized for the reduced models, and therefore, they are not equilibrium geometries. Reoptimization would flatten the curved carbon part of the configurations. We want to maintain the curvature of the carbon part since curved geometries are expected to be more reactive and we expect that will be important for the binding of adsorbates. Secondly, the physics of our finite, curved configurations is different than that of a full carbon nanotube. In particular, the electrostatic moments will be different for an open, curved piece of carbon compared to a closed tube. Finally, the π -bonding interactions relative to a full tube can be different since the π bonding network has been truncated. Because of all these differences, the binding energies we obtain directly from the QMC energies of the models do not represent the true binding of two NO_2 molecules to complete carbon nanotubes. Our principal objective is not to determine that true binding from these calculations, but rather to compare methods typically used for these types of systems and to determine their relative accuracy on a simplified model. We will however use results from these models to make estimates of the binding energies to complete carbon nanotubes. To do that, we will assume that most of the effects that are missing from the reduced models can be estimated from the difference of the DFT energies obtained from the reduced models and the complete CNT,

$$E_{\text{DMC,CNT}} = E_{\text{DMC,model}} + E_{\text{DFT,CNT}} - E_{\text{DFT,model}}, \quad (4)$$

where the DFT energies are computed using the same exchange–correlation functional and the same quality basis set. This type of extrapolation formula has been previously used in various contexts (see, e.g., [23]).

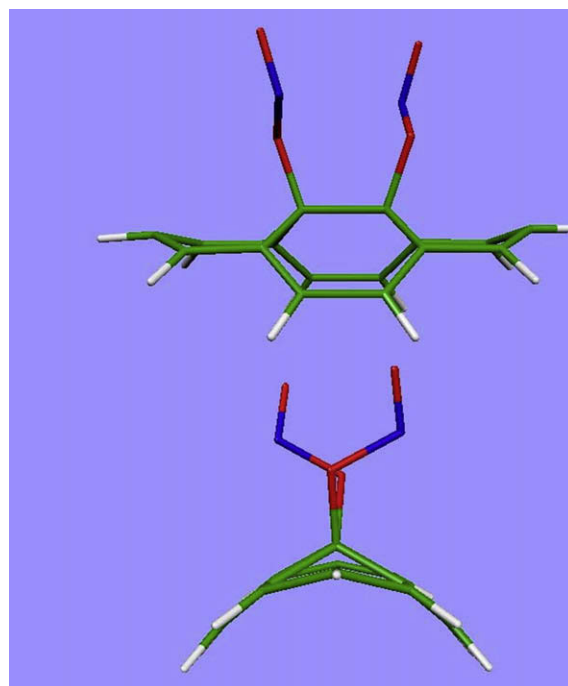


Fig. 2. Bonding configuration for NO_2 called ‘Odown’ where the O atoms are bonded to the nanotube model fragment.

4. Results

We performed all-electron DFT calculations using the LDA [24], PW91 [25], BPW91 [26,25], and B3LYP [26–30] functionals and MP2 calculations. We employed both the 6-31G* basis set as well as the larger correlation consistent cc-pVTZ basis set, and used the GAMESS [17] and GAUSSIAN03 packages [31]. For all DFT functionals, we repeated the calculations with the cc-pVQZ basis, which yielded binding energies compatible with the cc-pVTZ results to better than 1 kcal/mol. Therefore, the DFT/cc-pVTZ calculations are already well converged with respect to the basis set. The DFT and MP2 results are collected in Table 1, where we use the convention that bound systems have positive binding energies.

We first analyze the results obtained with the small 6-31G* basis set and note that our B3LYP and MP2 results with this basis set reproduce those reported in Ref. [2]. While both MP2 and B3LYP do not bind the adsorbates, MP2 gives considerably more binding than B3LYP (20 kcal/mol more for Ndown and 11 kcal/mol for Odown). The BPW91 and B3LYP binding energies are similar, while PW91 (which was used in the periodic calculations of Ref. [4]) is found to bind more strongly than B3LYP by 15 kcal/mol for Ndown and 10 kcal/mol for Odown. In contrast to other functionals and MP2, LDA yields a positive binding energy for both Ndown and Odown, and a binding for Ndown which differs from the B3LYP value by almost 50 kcal/mol. Finally, we note that the Ndown/Odown energy difference (denoted by Δ in Table 1) changes sign depending on the method. The sign of Δ indicates the preferred bonding geometry, with B3LYP, BPW91, and PW91 favoring Odown whereas MP2 and LDA favor Ndown.

We find that some of these differences become even more pronounced when using the larger cc-pVTZ basis set. In particular, the B3LYP, BPW91, PW91, and LDA binding energies decrease by 7–8 kcal/mol for both bonding configurations while the MP2 numbers change by only about 1 kcal/mol. The significant difference between the B3LYP and LDA energies persists with the larger basis set, and is therefore due to the approximate treatment of electron correlation. The cc-pVTZ results also suggest that DFT calculations with the small 6-31G* basis set on full nanotube geometries [2] may have a similarly strong basis set dependence.

In Table 1, we include Hartree–Fock (HF), B3LYP, and MP2 calculations performed using the same ECP and basis sets as for the QMC computations. The HF binding energies of –69 kcal/mol for Ndown and –48 kcal/mol are considerably less than the values obtained with B3LYP and MP2 indicating that correlation effects are important. From the Δ values, we note that HF favors Odown by 21 kcal/mol, B3LYP favors Odown by 6 kcal/mol, while MP2 favors Ndown by 5 kcal/mol. The B3LYP and MP2 binding energies using the ECP agree with the all-electron numbers using the cc-pVTZ basis set. The corresponding total energies are included for comparison with the QMC total energies in Table 2.

Table 2

Total energies (Hartrees) for the Ndown and Odown composites and the pyrene and NO₂ fragments. The statistical error on the QMC total energies is 1 mHartree.

	Ndown	Odown	Pyrene	NO ₂
<i>ECP calculations</i>				
HF	–175.951	–175.984	–93.918	–41.072
B3LYP	–180.033	–180.044	–96.454	–41.819
MP2	–179.612	–179.605	–96.240	–41.693
<i>Single determinant/ECP QMC</i>				
VMC	–180.002	–179.981	–96.522	–41.760
DMC	–180.306	–180.308	–96.705	–41.816
<i>Multi CSF/ECP QMC</i>				
VMC	–180.011	–179.996		
DMC	–180.314	–180.318		

In addition to B3LYP and MP2 calculations, RB [2] performed CCSD(T) calculations using the 6-31G* basis set. Due to the large system sizes, the Ndown and pyrene geometries were symmetrized, and B3LYP, MP2, and CCSD(T) calculations were performed with these new structures. Since the symmetrized geometries are different from the ones used in this work, our results are not strictly comparable to the CCSD(T) calculations. On the other hand, the effect of symmetrization does not appear to be large since the B3LYP binding energy changes by only –3 kcal/mol to a value of –32 kcal/mol while the MP2 value remains essentially unchanged at –9 kcal/mol [2]. The CCSD(T) calculation for Ndown gives –18.9 kcal/mol which lies between the PW91/cc-pVTZ and MP2/cc-pVTZ values. The CCSD(T) numbers are also included in Table 1 for comparison.

4.1. Single-determinant QMC

Single-determinant trial wave functions were constructed from Slater determinants of B3LYP orbitals multiplied by a Jastrow factor optimized by energy minimization. The Jastrow factor had 81 free parameters for Ndown and Odown and 43 parameters for pyrene and NO₂. The resulting binding energies and the total VMC and DMC energies are reported in Tables 1 and 2, respectively. Statistical errors are less than 1 mHartrees for the total energies and less than 1 kcal/mol for the binding energies.

From the total energies in Table 2, we observe that QMC has gained considerable correlation energy relative to HF both at the VMC and the DMC level. However, we also note from Table 1 that VMC and DMC yield significantly different binding energies as well as Ndown/Odown energy differences. In particular, while VMC favors Ndown by 13 kcal/mol, DMC stabilizes the binding energies to –19.4 kcal/mol for Ndown and –18.2 kcal/mol for Odown. The DMC energy difference between the Ndown and Odown configurations is compatible with zero within statistical error and, therefore, one bonding configuration is not preferred over the other.

If we compare the DMC binding energies with the DFT/cc-pVTZ and the MP2/cc-pVTZ results, we note that PW91 gives the best agreement with DMC, yielding roughly 3 kcal/mol less binding than DMC. Larger differences are seen with BPW91, B3LYP, MP2, and especially LDA which binds Ndown and Odown more strongly than DMC by 30 and 22 kcal/mol, respectively. It is also interesting to note that the DMC number for the binding of Ndown agrees very well with the CCSD(T) value of –18.9 kcal/mol obtained by RB using the symmetrized geometries and the smaller 6-31G* basis set.

In the DMC calculations we used a time step of $\Delta\tau = 0.1$ Hartree^{–1}. To assess the time-step error we did additional calculations for $\Delta\tau = 0.05$. The binding energy changes were on the order of 1 kcal/mol, comparable to the statistical uncertainty on the energies.

4.2. Multi-CSF QMC

Calculations using multi-CSF trial wave functions were performed in order to reduce the DMC fixed-node error. The multi-CSF wave functions are needed for a good description of static (near-degeneracy) correlation, whereas the Jastrow factor and the DMC projection take care of the dynamic correlation. For small systems, it is feasible to perform multiconfiguration self-consistent field (MCSCF) calculations with a complete active space (CAS), i.e., to include all the CSFs that can be obtained from excitations from a certain number of active orbitals. Such wave functions, with CSF coefficients reoptimized in the presence of the Jastrow factor, yield good DMC binding energies [8], but they are not feasible for systems as large as those in this Letter.

For the composite systems, Ndown and Odown, we first did a restricted CAS(24,24) (24 electrons distributed among 24 orbitals) calculation where we considered only singles and doubles excitations. To reduce the computational burden, we retained only the 7 CSFs (17 determinants) with coefficients larger than 0.0545. The MCSCF orbitals optimized for full expansions are not always better than the B3LYP orbitals when used in the truncated expansion and in the presence of a Jastrow factor. So, we used B3LYP orbitals for constructing the QMC wave functions; the CAS calculation was employed only to select the important CSFs. The CSF and Jastrow coefficients were optimized simultaneously. We do not expect these truncated wave functions to give reliable binding energies, but they can be used to compare the Ndown and Odown total energies.

As can be seen from Table 2 including additional CSFs improved the VMC energies by 9 and 15 mHartrees, and the DMC energies by 8 and 10 mHartrees for Ndown and Odown, respectively. As shown in Table 1, the difference between the Odown and Ndown multi-CSF DMC energies is 2.5 kcal/mol while the difference between the single-determinant DMC energies is 1.3 kcal/mol. The statistical error on both Ndown/Odown differences is 1 kcal/mol, so the single-determinant and multi-CSF DMC differences are both compatible with zero within less than a three-standard-deviation statistical error. Thus, the multi-CSF calculations confirm the single-determinant result for Δ .

4.3. Full tube binding energy estimates

Ricca and Bauschlicher [2] estimated the binding of two Ndown NO₂ molecules to a nanotube to be 16 kcal/mol for a (9,0) tube and 8 kcal/mol for a (10,0) tube. These values were computed starting from the B3LYP/6-31G* binding energies of -2 kcal/mol for the (9,0) and -10 kcal/mol for the (10,0) tube obtained in their small-cell PBC calculations. These DFT values were then corrected for the correlation error (13.7 kcal/mol estimated as the difference between the CCSD(T)/6-31G* and B3LYP/6-31G* calculations on the small symmetrized model) and the basis set error (3.8 kcal/mol estimated from MP2 calculations with 6-311G(2d,p) and 6-31G* basis sets).

In the same spirit, we can estimate a 'correlation correction' for the periodic B3LYP/6-31G* and BPW91/6-31G* calculations of the full nanotube reported in Ref. [2] and for the plane-wave PW91 calculation of Ref. [4]. We define this correction to be the difference between the DMC cluster binding energy and the cluster binding energies computed with the same DFT functional and the same quality basis set as in the full tube calculations Eq. (4). For example, for the periodic B3LYP/6-31G* calculation of Ref. [2], we obtain a correction of 9.7 kcal/mol, which yields an estimate for the binding of two Ndown NO₂'s to a nanotube of 8.1 kcal/mol for a (9,0) tube and -4.6 kcal/mol for a (10,0) tube. Note that RB used results from small cell (80 carbons) calculations to form their estimates. We on the other hand use their large cell (120 carbons) numbers which we expect to be slightly better for our updated estimates. Similarly, we can compute estimates for the BPW91/6-31G* [2] and the plane-wave PW91 [4] calculations. These results are collected in Table 3.

We note that the full tube calculation with PW91 and a plane wave basis binds more strongly for both the (9,0) and the (10,0) tube by 8 kcal/mol compared to B3LYP/6-31G* and BPW91/6-31G*. While different geometries and basis sets may explain some of the differences between these results, the fact that PW91 binds more strongly for the full tube is consistent with the trends we observe for the clusters.

Compared to the earlier calculations of Ref. [2], the correlation estimates derived from the present DMC calculations have the advantages of much smaller basis-set errors and of not employing

Table 3

Estimated binding energies (BE) (kcal/mol) of the Ndown configuration on a full CNT. We list the DFT binding energies from periodic-cell calculations, the QMC correlation corrections (see text for details), and estimates for the full tube binding energies.

	DFT BE	QMC correction	Estimated BE
<i>(9,0) Carbon nanotube</i>			
B3LYP/6-31G*	-1.6 [2]	9.8	8.2
BPW91/6-31G*	-4.1 [2]	6.6	2.5
PW91/plane wave	4.0 [4]	3.1	7.1
<i>(10,0) Carbon nanotube</i>			
B3LYP/6-31G*	-14.3 [2]	9.8	-4.5
BPW91/6-31G*	-14.2 [2]	6.6	-7.6
PW91/plane wave	-6.3 [4]	3.1	-3.2

the symmetrized model. Moreover, when using the plane-wave PW91 binding energies for the full nanotube [4] in combination with our PW91/cc-pVTZ results for the cluster, we have also largely eliminated the basis set error coming from the DFT calculations, which is instead present in the 6-31G* estimates. Unfortunately, we still use the extrapolation formula Eq. (4) to estimate the binding energy to the CNT, which certainly limits the accuracy of our final estimate as the correlation correction has been computed on relatively small cluster models. In fact, we expect the extrapolation scheme to work if the correlation correction is not too large and if the DFT binding energies computed on the fragments are not far from the infinite limit. The limitations of the extrapolation scheme in our case are apparent from Table 3 as the estimated binding energies have a non negligible spread. More accurate estimates would require QMC calculations on larger clusters or on the fully periodic system. Nevertheless, we see that the three estimates we derive from the different methods are roughly consistent, and it is therefore reasonable to conclude that the binding of two NO₂'s to a nanotube is very weak with a (9,0) tube binding more strongly than a (10,0) tube.

5. Conclusion

In this work, we used QMC to study the role of electronic correlations in a model system representing the adsorption of two NO₂ molecules to a carbon nanotube. Interest in this system is motivated by the observed two orders of magnitude change in the conductivity of the tubes after exposure to trace amounts of gaseous NO₂. We performed calculations using both single determinant and multi-CSF wave functions. Our calculated DMC binding energies for the model systems are -19.4 ± 1.2 kcal/mol for the Ndown configuration and -18.2 ± 1.2 kcal/mol for the Odown configuration which indicates that there is not a clearly preferred bonding configuration in these models. We find that basis set and correlations effects are important for these systems. In particular, compared with the QMC results, we find that MP2 and LDA overbind while B3LYP and BPW91 underbind. The PW91 functional gives the best agreement with the DMC results. Using these binding energies, we update previous estimates by RB [2] for the binding to the full tube. The weakness of the binding for the two NO₂ adsorbates puts the charge transfer mechanism in CNT molecular sensors in further doubt, and suggests that the conductivity change observed in these systems results from another mechanism.

Acknowledgements

J.W.L. and C.W.B. are civil servants in the TS Division (Mail Stop 229-1). This work was funded in part by grants from the NASA Ames DDF, European Marie Curie Outgoing International Fellowship (039750-QMC-DFT), the NSF and the DOE.

References

- [1] J. Kong, N. Franklin, C. Zhou, M. Chapline, S. Peng, K. Cho, H. Dai, *Science* 287 (2000) 623.
- [2] A. Ricca, C. Bauschlicher, *Chem. Phys.* 323 (2006) 511.
- [3] W.L. Yim, X. Gong, Z. Liu, *J. Chem. Phys.* 107 (2003) 9363.
- [4] Y. Zhang, S. Chiuho, Z. Liu, J. Li, *J. Phys. Chem. B* 110 (2006) 22462.
- [5] G. Cicero, J. Grossmann, G. Galli, *Phys. Rev. B* 74 (2006) 035425.
- [6] W.M.C. Foulkes, L. Mitas, R.J. Needs, G. Rajagopal, *Rev. Mod. Phys.* 73 (2001) 33.
- [7] M.P. Nightingale, C.J. Umrigar (Eds.), *Quantum Monte Carlo Methods in Physics and Chemistry*, NATO ASI Series C 525, Kluwer, Dordrecht, 1999.
- [8] J. Toulouse, C. Umrigar, *J. Chem. Phys.* 128 (2008) 174101.
- [9] C.J. Umrigar, C. Filippi, *Phys. Rev. Lett.* 94 (2005) 150201.
- [10] J. Toulouse, C.J. Umrigar, *J. Chem. Phys.* 126 (2007) 084102.
- [11] C.J. Umrigar, J. Toulouse, C. Filippi, S. Sorella, R.G. Hennig, *Phys. Rev. Lett.* 98 (2007) 110201.
- [12] C.J. Umrigar, K.G. Wilson, J.W. Wilkins, *Phys. Rev. Lett.* 60 (1998) 1719.
- [13] C.J. Umrigar, *Phys. Rev. Lett.* 71 (1993) 408.
- [14] N. Metropolis, A.W. Rosenbluth, M.N. Rosenbluth, A.H. Teller, E. Teller, *J. Chem. Phys.* 21 (1953) 1087.
- [15] W.K. Hastings, *Biometrika* 57 (1970) 97.
- [16] C.J. Umrigar, M.P. Nightingale, K.J. Runge, *J. Chem. Phys.* 99 (1993) 2865.
- [17] M.W. Schmidt et al., *J. Comput. Chem.* 14 (1993) 1347.
- [18] S. Sorella, M. Casula, D. Rocca, *J. Chem. Phys.* 127 (2007) 014105.
- [19] We used the code of E. Shirley to generate norm-conserving Hartree–Fock pseudopotential with the construction by D. Vanderbilt *Phys. Rev. B* 32 (1985) 8412.
- [20] D. Vanderbilt, *Phys. Rev. B* 32 (1985) 8412.
- [21] L. Mitas, E.L. Shirley, D.M. Ceperley, *J. Chem. Phys.* 95 (1991) 3467.
- [22] T.H. Dunning, *J. Chem. Phys.* 90 (1989) 1007.
- [23] S. Humbel, S. Sieber, K. Morokuma, *J. Chem. Phys.* 105 (1996) 1959.
- [24] S.H. Vosko, L. Wilk, M. Nusair, *Can. J. Phys.* 58 (1980) 1200.
- [25] J. Perdew, Y. Wang, *Phys. Rev. B* 45 (1991) 13244.
- [26] A.D. Becke, *Phys. Rev. A* 38 (1988) 3098.
- [27] C. Lee, W. Yang, R.G. Parr, *Phys. Rev. B* 37 (1988) 785.
- [28] A.D. Becke, *J. Chem. Phys.* 98 (1993) 5648.
- [29] V. Barone, C. Adamo, *Chem. Phys. Lett.* 224 (1994) 432.
- [30] P.J. Stephens, F.J. Devlin, C.F. Chabalowski, M.J. Frisch, *J. Phys. Chem.* 98 (1994) 11623.
- [31] M.J. Frisch, et al., *GAUSSIAN 03*, Revision B.05, Gaussian, Inc., Pittsburgh PA, 2003.